UNIVERSITI MALAYSIA PERLIS

UniMAP

Synthesis, Characterization and Visible Light/NIR Photodetector of CuO Nanowires Fabrication

Abdul-Qader D. Faisal[1] and Wafaa K. Khalef[2]

[1,2]*Applied Science Department/University of Technology/Baghdad/Iraq.*

ABSTRACT

This works successfully synthesized vertically aligned, high density, long, large aspect ratio of CuO nanowires (CuO NWs) via thermal oxidation of copper (Cu) foil with atmospheric air. The oxidation process was conducted under temperature and time variation. The morphology and structure properties of CuO NWs were investigated by scanning electron microscope (SEM) and X-ray diffraction (XRD) respectively. UV-Visible spectrophotometer was also used to estimate the direct band gap (1.75eV) from the transmission spectrum. Furthermore, the film exhibit high absorption in the visible range and near infrared wavelength. The optimized parameters for long, small diameter, high density of CuO NWs at oxidation temperature of 500ºC for 6-8h in the atmospheric air were found. The diameter and length of CuO NWs was determined within the range of 50-100 nm and 20-30 μm respectively. These optimized properties of CuO NWs make it a dependable candidate for visible light/ near-infrared (NIR) photodetector fabrication. Therefore, the photodetector measurements were proved to render an acceptable performance.

Keywords: Thermal Oxidation, Copper Oxide Nanowires (CuO NWs), Visible Light/NIR, Photodetectors.

1. INTRODUCTION

One-dimensional metal-oxide semiconductor nanostructures such as whiskers and nanowires receive increasing interest due to their unique properties and variety of potential applications [1-4]. Among the metal oxides, cupric oxide (CuO) has been extensively studied as a p-type semiconductor. CuO has a direct band gap in the range of 1.2 to 2.0 eV and exhibits many excellent chemical and physical properties [5, 6]. After the first discovery of CuO whiskers [7], various growth techniques have been developed to synthesize CuO nanostructures such as hydrothermal method [8], wet chemical method [9], thermal oxidation [10,11] and the template based sol-gel route [12]. Among these techniques, thermal oxidation is an interesting technique because it is simple, cheap and produces high quality nanowires (NWs). Many researchers have reported on the growth of CuO nanowires (CuO NWs) by a thermal oxidation technique [13.14]. Various structures and shapes of copper oxide nanostructures have been investigated which includes: nanowhiskers [15], nanowires [16], flower-like [17], nanoneedles [18], nanorods [19], nanotubes [20], nanocrystals [21], nanosheets [22], and nanoribbons [23]. Nanostructured CuO materials, especially 1D CuO NWs, have received much more attention for some application such as field-effect transistors [24], gas sensors [25], UV light sensing [26], visible light photodetector [27], IR photodetector [28,29], and UV/IR photodetector [30,31].

Corresponding Author: drwafaa1980@gmail.com

Other materials such as CdS NPs dopted with copper and their analysis as p-Cds/n-ZnO synthesized as a thin film photodiode has been used in a photodiode application [32]. Furthermore, metal oxide composite was also fabricated as a photodiodes [33]. Graphene-organic semiconductor hybrid were also fabricated as materials for new photodiodes device [34]. In this work, the successful growth of vertically aligned CuO NWs of copper foil thermally

oxidize in atmospheric air using tube furnace were presented. The surface morphologies and crystal structures of CuO NWs produced at different oxidation temperature and time were investigated. The optimum growth temperature of vertically aligned CuO NWs produced via thermal annealing of copper foil was determined. Besides the synthesis and characterization of CuO NWs, their performance as a photodetector fabrication for visible light/near-infrared (NIR) was also investigated.

2. EXPERIMENTAL DETAILS

2.1 Thermal Oxidation

Before the CuO nanowires (CuO NWs) growth, pieces of commercial grade copper foils (20mm×20mm×0.2mm) were washed with soap solution. The foils were then washed again with dilute hydrochloric acid to remove the native oxide layer, then rinsed in deionized water and followed by cleaning with acetone, ethanol, and deionized water under an ultrasonic bath for 15 min. Then, the foils were finally dried with nitrogen (N2) flow. The thermal oxidation process of the foil was conducted in a single zone tube furnace with quartz tube (5cm diameter, 100cm long). The cleaned copper foils were loaded on alumina boat for each step of temperature and inserted into the middle of the quartz tube. The tube furnace was heated to the set-point temperature of 450ºC, 500ºC, and 550ºC at atmospheric pressure and with time variation. The furnace then switched off and allowed to cool naturally to room temperature to prevent the film from cracking by thermal stress by air. The sample was pulled out of the furnace for further characterization.

2.2 Characterizations

X-ray diffraction data of the CuO powder were obtained by using a Shimadzu XRD-6000 X-ray diffractometer working with Cu Kα radiation (λ = 1.5406 Å) and scanned with speed of 12° min^{-1} and the diffraction angle ranges from 20° to 80°. The morphology of the films was imaged with Scanning Electron Microscope (Inspect S50, FEI Company, Netherland). UV-Visible spectrophotometer (UV-Vis T80/PG Instrument Ltd) was used for optical properties calculation.

3. RESULTS AND DISCUSSION

3.1 Morphological Analysis

The CuO NWs morphology was investigated at different oxidation temperatures of 450ºC, 500ºC, and 550ºC and time of 2-4h. Figure 1 shows the scanning electron microscope (SEM) images of CuO NWs growth process monitoring. The nanowires started to grow with minor distributed nanowires at a temperature of 450ºC for 2h as shown in Figure 1(a). Figure 1(b) shows the nanowires growth increased at the same temperature for 4h. When the temperature is increased to 500ºC for 2 and 4h, the nanowire was grown with increasing density and length as shown in Figure 1(b) and 1(c) respectively. As the temperature increased to 550ºC for 2h and 4h, the lower density of nanowires growth was found as shown in Figure 1(e) and 1(f) respectively.
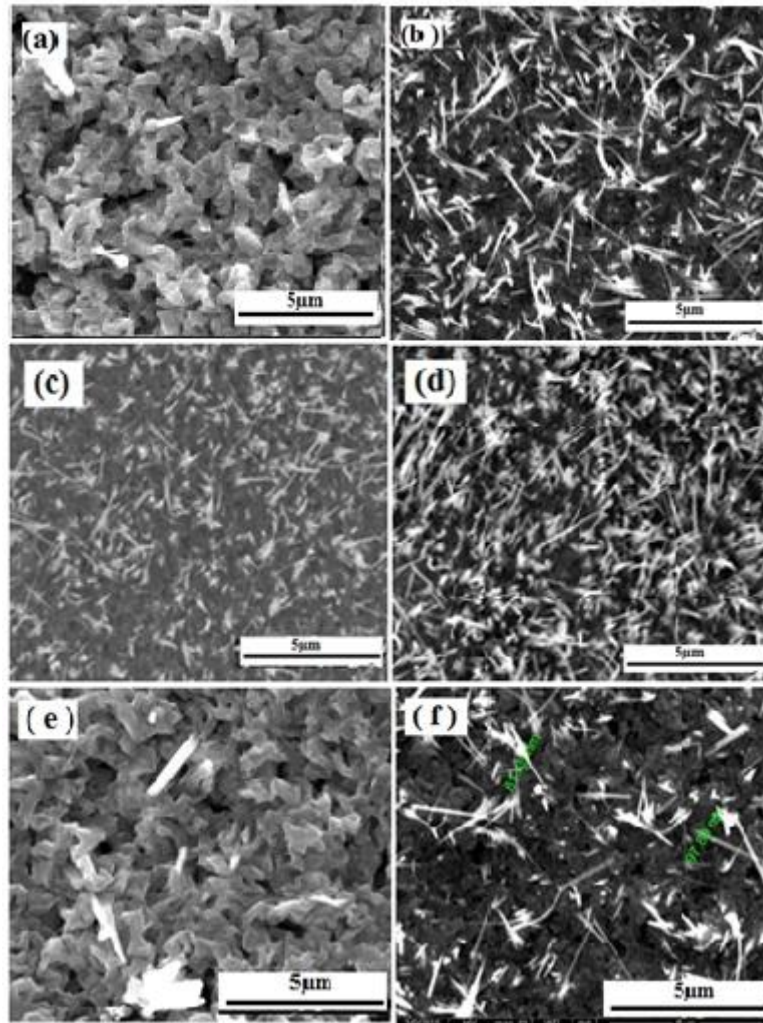
Figure 1. SEM images of CuO NWs grown at various temperatures and times (a,b) 450ºC,2h,4h; (c,d) 500ºC,2h,4h; (e,f) 550ºC, 2h,4h.

Figure 2 shows the top view (a and c) and tilted 40º (b and d) of SEM images for the typical as-synthesized CuO nanowires. Figure 2(b) and 2(d) images revealed a long, thin, and vertically aligned CuO nanowires on the substrate surface. The measured sizes of these wires are between 100 and 150 nm in diameter and its length is greater than 10µm. Two different diameters can be observed along the wires. The bottom half diameter is the vertically aligned wires which were previously measured. The second top half is the long, uniform, crossing over and fine diameters of the nanowires, which could be having a large aspect ratio.
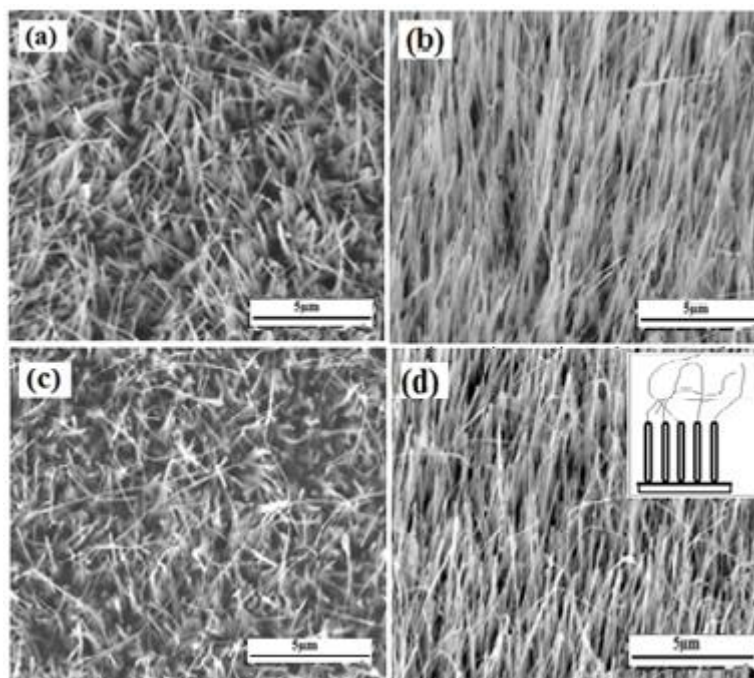
Figure 2. SEM images of as-synthesized CuO NWs grown at constant temperature and various times. (a,b) 500ºC , 6h; (c,d) 500ºC, 8h respectively.

The benefit of this work is to obtain CuO NWs with diameters range of 50-100 nm and 10-20 μm long (large aspect ratio about 500). Vertical CuO nanowires were grown in a simple oxidation process. This product is controllable and scalable for some application. The optimum temperature and time needed in order to grow vertically aligned CuO NWs from copper foil is 500ºC and 6-8h respectively.

3.2 Structural Analysis

Figure 3(a) and 3(b) show a typical XRD pattern of the copper foil oxidized at 500ºC for 6h and 8h respectively in atmospheric air. It can be seen that there are two phases of copper oxide in both figures. These phases are indexed as CuO and Cu_2O relative to the PDF files No. 05-0661 and 05-666 respectively. Figure 3(a) shows the XRD pattern of copper foil oxidized at 500ºC for 6 hours. In this figure, Cu_2O peaks are the dominant compared to the CuO peaks. This is because, during the Cu foil oxidation, Cu_2O film was firstly formed before the growing of the CuO NWs. Figure 3(b) shows the XRD pattern of copper foil oxidized at 500ºC for 8 hours. Mixed phases are also observed in this figure for CuO and Cu_2O with higher intensity of CuO. Therefore, it is possible to fabricate visible light photodetector based on the preferred and dominated CuO NWs structure shown in Figure 3(b).

The mechanism of CuO NWs grown by an oxidation process of Cu foil is explained in three steps. In the 1st step, the existing hillocks relieve the compressive stress created at the Cu foil at a certain temperature and time in the air. In the 2nd step, Cu_2O is formed by the oxidation of the top surface in air ambient. In the 3rd step, the transformation of the Cu_2O to the CuO NW. Therefore, the main sources of CuO NW growth are the continuous feeding of Cu from the copper foil and oxygen (O_2) from the ambient air.
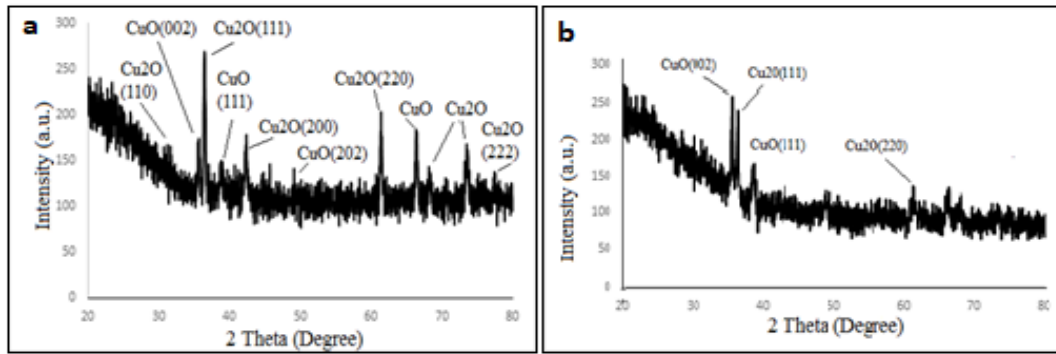
Figure 3. XRD pattern of CuO NWs grown at 500ºC for 6h (a), 8h (b) in atmospheric air.

3.3 Optical Properties of CuO NWs

Generally, the optical properties of the film depend on many factors such as crystal structure, incident photon energy, film thickness, and film surface morphology [28]. The optical gap of CuO NWs was calculated using Eq. 1 [35]:

$$(hv) = \beta(hv - Eg)^n/\alpha \tag{1}$$

Where hv is the incident photon energy, α is the absorption coefficient, β is a material dependent constant and Eg is the optical energy gap. The value of *n* depends on the nature of the transition. This value takes 1/2, 3/2, 2 or 3 for direct allowed, direct forbidden, indirect allowed indirect forbidden transitions respectively[36]. The usual method of determining Eg involves plotting $(\alpha hv)^{1/n}$ versus hv.

Figure 4(a) and 4(b) shows the relation of CuO NWs transmittance versus the wavelength, synthesized at 500ºC for 6h and 8h in atmospheric air. The average transmittance of both curves is found around 60-80% in visible and IR regions (500nm-1100nm) and higher. The insets in Figure 4(a) and 4(b) display the relation between $(\alpha hv)^2$ and the photon energy (hv) for which its oxidized at 500ºC for 6h and 8h in atmospheric air, respectively. The direct energy gap values of 2.1 and 1.6 eV for Cu_2O and CuO NWs were calculated respectively. These low band gap values exhibit a broadband photo response in the visible/ IR region. The obtained band gap values for Cu_2O and CuO are within the ranges of (2.10eV - 2.61eV) and (1.20 eV - 2.10eV) respectively as reported by [37,38].These optical properties are in a good agreement with reported results from other studies [28, 39].
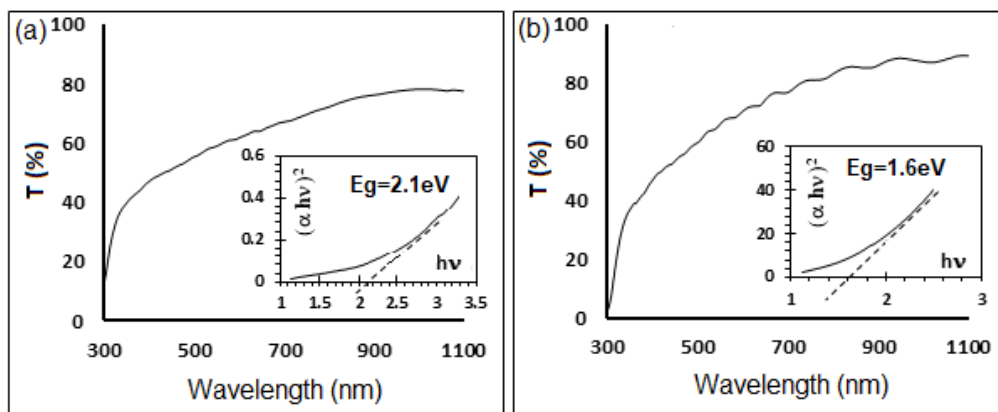

Figure 4. (a) Transmittance for CuO NWs synthesized at 500ºC for 6h(a) and 8h (b). The insets are represent a corresponding energy gap calculations.

4. CuO NWs BASED VISIBLE LIGHT PHOTODETECTOR FABRICATION

For the fabrication of the photodetector, the sample was prepared by peeling the copper metal using fine razor and fixed on a glass slide. Silver paste was used to form solid contact pads on the top of the detector at both ends of the film only. The glass slide was left in the oven to dry at 100ºC for 30 minutes. Figure 5(a), 5(b), and 5(c) demonstrate the photodetector device assembly. The detector device was then placed on an insulated sheet in the ambient atmosphere. The light intensity was varied using a variable transformer (AC) and measured with the power meter (Sanwa /Mobiken-Laser power meter LP1). Other instruments such as DC power supply (LONG WEI PS-305DM-China), precise digital timer (Sports timer /Germany), 100watt white light source (Halogen) and manual light switch were used for experimental measurements. The optical power supplied to the light source was varied through variable resistance (Variac). The experimental data were collected with a laptop connected and pre-installed to Fluke 8846A Digital Multimeter. Figure 5a shows the schematic of the detector device. The sample was fixed under pre-calibrated visible light source as shown in Figure 5(b). The effective area of the CuO NWs exposed to the light shown in Figure 5(c) was calculated approximately 0.24cm^2.

The current-voltage characteristics of the photodetector device for CuO NWs on glass measured in the dark and at ambient atmosphere is shown in Figure 5(d). The linear curve observed has a high slope of 5 M Ω. There is a minor nonlinear behavior observed around 0 volts (< 0.5v) as explained in the inset of Figure 5(d). This behavior is due to the Schottky barrier between CuO NWs and the silver electrode. The outcomes indicate that an ohmic contact is established between the silver electrode and the Cu wire.
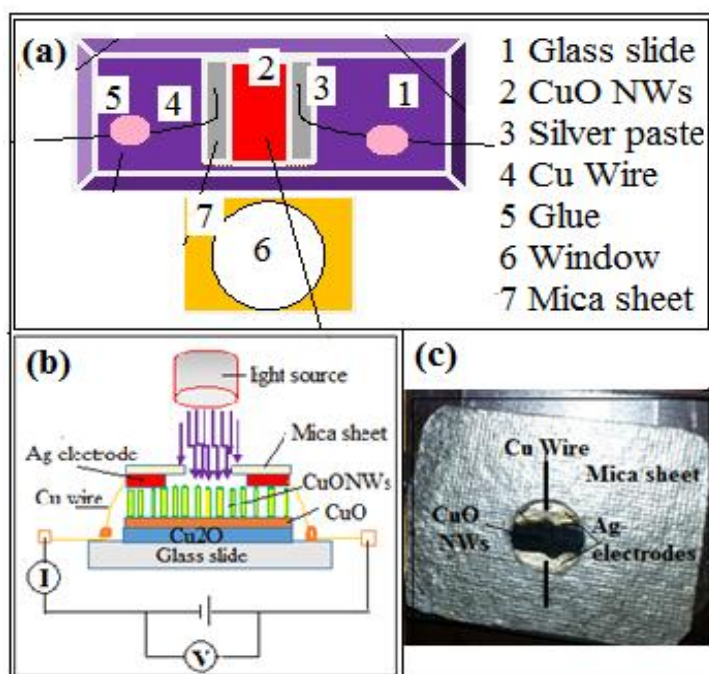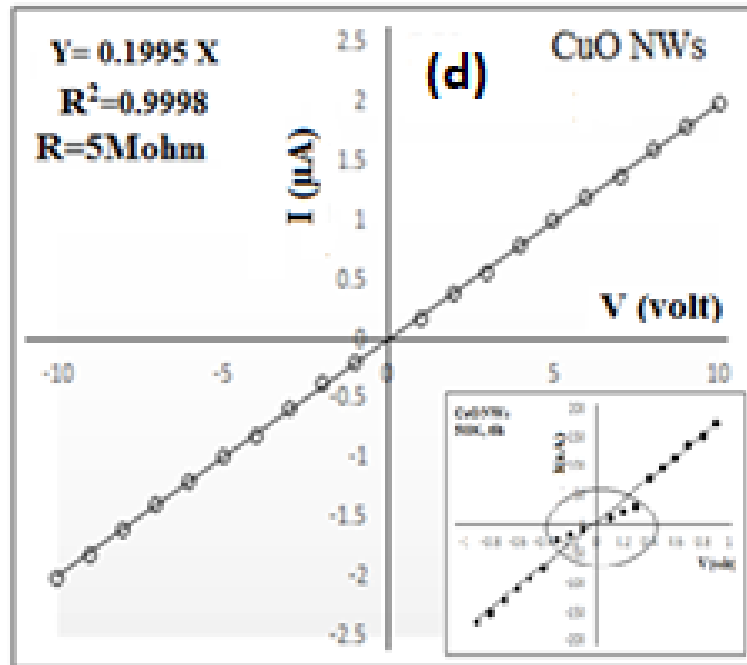
Figure 5. Photodetector of CuO NWs (a) Schematic of the device assembly; (b) Setup measurement diagram; (c) Photograph of the detector device; (d). Current-voltage (I-V) curve in the dark.

4.2 Photodetector Performance

In the present work, CuO NWs on the slide glass substrate was studied as a photo-detector at room temperature and atmospheric air. The photoresponse of the CuO NWs detector proved to have a good response to visible light. Figure 6(a) shows the I-V curves of the device under visible light irradiation with decreasing light intensity from 166mW/cm^2 to 0.3mW/cm^2. The I-V curves also reveals an ohmic behavior with good linearity. In addition, as the incident light intensity decreased, the maximum current value also decreased from 9µA and lower at the bias voltage of 5 volts. The photocurrent within 1µA was measured in the dark at 5 volts. Therefore, the calculated sensitivity range of this detector [S (%) = (I_{phot}-I_{dark}) / I dark] is varied from 100-800, which is quite acceptable compared with results from other previous works [40]. The photocurrent (I) versus light intensity has been described as a power law [41]:

$$I = A * P^b \tag{2}$$

Where I is the photocurrent; A is proportionality constant; P is the light intensity, and b is the empirical value. Figure 6(b) shows the relation between the photocurrent I (µA) as a function of light intensity P (mW/cm^2). By fitting the measured data (Experimental-solid dark line) with the power law, the intensity law, I =1.4*P$^{0.34}$ was obtained, where I is the photocurrent and P is the light intensity. The none unity exponent (b=0.34) is a consequence of the complex process of (electron-hole) generation, trapping and recombination within the semiconductor [42].
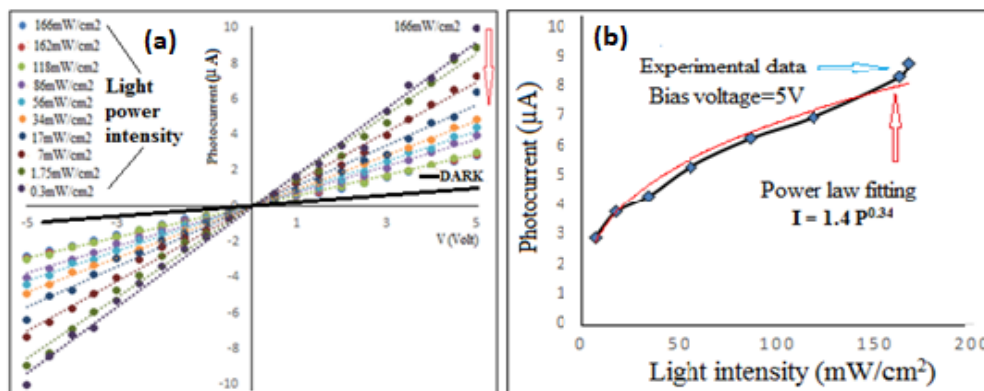
Figure 6. (a) I-V curves for the detector exposed to the light at various power densities (Black solid line represents: dark current); (b) Light intensity dependence of the photocurrent measured at 5 v bias voltage (black solid line). The red solid line is the fitting results.

Figure 7 explains the time dependence photoresponse of this device measured under the fixed visible light intensity of 166mW/cm^2 at various voltages (1-5volts). These curves are evaluated by manual ON/OFF cycles. Figure 7(a) represent the photocurrent variation following the incident light switching between ON and OFF cycles. This indicates that the detectable response is acceptable for this device. Moreover, an excellent device performance was confirmed by their stability and reversibility at the measured ON/OFF cycles. Moreover, the curves in Figure 7(b) explained the time dependence photoresponse at the fixed bias voltage of 5 volts and variable visible light intensity ranging from 166mW/cm^2 to 42mW/cm^2. Figure 7(c) clearly shows the time dependence photoresponse at fixed values of a bias voltage of 5 volts and power intensity of 166mW/cm^2. Figure 7(d) shows ON/OFF for two cycles, where the rise and decay time are counted within the 40s and 50s respectively, which are compared with results from other works [43].
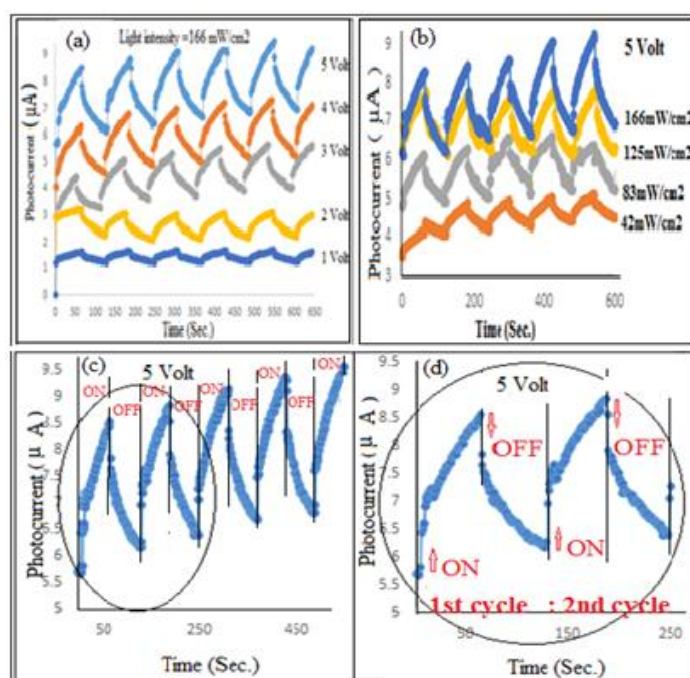

Figure 7. Time-dependent photocurrent response for CuO NWs; (a) at various voltages and fixed light intensity of 166mW/cm^2; (b) at various light intensity and fixed bias voltage of 5 volts; (c and d) Multiple and double photocurrent response cycles at the light intensity of 166 mW/cm^2 and biased voltage of 5volt respectively.

4.3 Photodetector Evaluation

There are two important parameters that need to be taken into consideration in order to enable the photodetector to determine the sensitivity for optoelectronic applications which are spectral responsivity (R_λ) and quantum efficiency (η). They are described in Eq. 3 and Eq. 4 [44]:

$$R_\lambda = \Delta I/PA \qquad (3)$$

$$\eta = hcR_\lambda/e\lambda \qquad (4)$$

Where ΔI ($\Delta I = I_{photo} - I_{dark}$) is the photocurrent and the dark current difference, P is the light power intensity irradiated on the CuO NWs, A is the effective area of the irradiated sample, h is the photocurrent, c is the velocity of light, h is the Planck's constant, e is the electronic charge, and λ is the exciting wavelength.

The plot in Figure 8(a) and 8(b) show the relation between the spectral responsivity and the quantum efficiency as a function of the wavelength of constant bias voltage (5 volts) of the CuO NWs prepared by thermal oxidation of copper sheet. Regarding these results, the device exhibits high responsivity (0.25 A/W) for visible light at 500nm and 0.39 A/W for IR light at 1000nm as shown in Figure 8(a)

The quantum efficiency (η) is an important evaluation parameter for photodetector performance. It is related to the number of electron-hole pairs excited by absorbed photons [28].The quantum efficiency values of CuO NWs photodetector (refer Figure 8(b)) are 62% (at 500nm) and 48% (at 1000nm). These values suggest that the synthesized CuO NWs exhibited a high detection performance to visible light and IR.
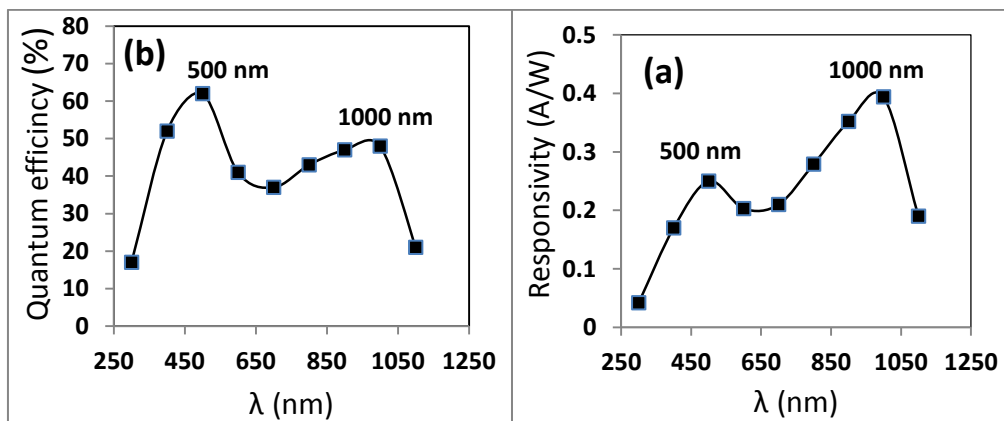

Figure 8. Calculated the photodetector parameters for CuONWs at visible to IR (a) responsivity (R); (b) quantum efficiency (η%) vs. wavelengths.

5. CONCLUSIONS

In summary, this works have successfully synthesized CuO NWs via a thermal oxidation method at various temperatures and time. Optimized growth parameters to grow CuONWs were determined. The optimized temperature and time values to grow nanowires were 500°C and 6-8h respectively. The diameter of the length of CuO NWs was determined within the range of 50-100 nm and 20-30 μm respectively. The high aspect ratio (L/D) of nanowires could be a serious benefit for many applications. The as-synthesized CuO NWs revealed high sensitivity to visible light/IR irradiation in the wavelength range of the 400nm-1000nm. A CuO

NWs photodetector device was fabricated and this device exhibits a reasonable sensitivity. I-V curves under dark and light response were investigated. Upon visible light illumination, the detector exhibits high sensitivity at 400-1000nm with different bias voltages at room temperature and in air atmosphere. In conclusion, the developed CuO NWs photocurrent detector in this research is quite promising as a visible/NIR light detector fabricated for some applications.

REFERENCES

[1]   Y. J. Choi, I. S. Hwang, J. G. Park, K. J. Choi, J. H. Park, J. H. Lee, "Novel fabrication of an SnO_2 nanowire gas sensor with high sensitivity," Nanotechnology **19** (2008) 1-9.

[2]   S. Hullavarad, N. Hullavarad, D. Look, B. Claflin, "Persistent photoconductivity studies in nanostructured ZnO UV Sensors," Nanoscale Res Lett **4** (2009) 1421–1427.

[3]   K. Wang, J. Ruan, H. Song, J. Zhang, Y. Wo, S. Guo & D. Cui," Biocompatibility of graphene oxide,"Nanoscale Res. Lett. **6** (2011) 1- 8.

[4]   A. E. Rakhshani, "Preparation, characteristics and photovoltaic properties of cuprous oxide:A review," Solid-State Elect. **29** (1986) 7-17.

[5]   P. R. Shao, S. Z. Deng, J. Xu, N. S. Chen, "A cylindrical core-shell-like TiO_2 nanotube array anode for flexible fiber-type dye-sensitized solar cells,"Nanoscale Res. Lett. **6** (2011) 94-98.

[6]   S. Sumikur, S. Mori, S Shimizu, H. Usami, E. J. Suzuki, "Photoelectrochemical characteristics of cells with dyed and undyed nanoporous p-type semiconductor CuO electrodes," Photochem. Photobiol. A **194** (2008) 143-147.

[7]   F. R. N. Nabarro & J. P. Jackson, Growth of whiskers: A review perfection of crystal growth, New York, (1958).

[8]   C. F. Alison, J. Joe, "Hydrothermal synthesis and characterization of copper oxide flower-like nanostructures," Elixir Nanocomp. Mater. **50** (2012) 10541-10543.

[9]   M. Pal, U. Pal, J. M. G. Y Jimenez & F. Pérez-Rodríguez, "Effect of crystallization and dopant concentration on the emission behaviour of TiO_2:Eu nanophosphors, "Nanoscale Res. Lett. **7** (2012) 1-12.

[10] J. T. Chen, F. Zhang, G. A. Zhang, B. B. Miao, X. Y. Fan, P. X. Yan,"CuO nanowires synthesized by thermal oxidation route,"J. of. Alloys and Comp. **454** (2006) 268-273.

[11] S.-L. Cheng & M.-F. Chen, "Fabrication, characterization, and kinetic study of vertical single-crystalline CuO nanowires on Si substrates,"Nanoscale Res. Lett. **7**, 1 (2012) 119-125.

[12] Y. S. SU, Y. Cheng-min, L. I. Ang-Hai-tao, G. A. Hlin, O. Hong-jun Trans, "Controlled synthesis of highly ordered CuO nanowire arrays by template-based sol-gel route," Trans. Nonferr. Met. Soc. China **17** (2007) 783-786.

[13] B. J. Hansen, G. Lu & J. Chen, "Direct oxidation growth of CuO nanowires from copper-containing substrates,"J. of Nanomater. **48** (2008) 1-7.

[14] L. N. Jianbo, K. S. Tetsuo, J. Takashi, "The synthesis of highly aligned cupric oxide nanowires by heating of copper foil, "J. of Nanomater. **1** (2011) 1-8.

[15] W. Wenzhong, Z. Yongjie, W. Xiaosh, W. Guanghou, "Synthesis and characterization of CuOnanowhiskers by a novel one-step, solid-state reaction in the presence of a nonionic surfactant, "Mater. Res. Bull. **37** (2002) 1093-1100.

[16] K. Manmeet, M. Kunal, C. Shipra, B. Jung, V. Neetika, "Growth and branching of CuO nanowires by thermal oxidation of copper, "J. of Cryst. Growth **289** (2006) 670-675.

[17] T. FeiVitae, Y. Wenqing Vitae, Z. Youfei Vitae, M. Yutao, T. Vitae Yang Vitae, X. Tongguang Vitae, L. Shuhui Vitae, Z. Yongfa, "Size-induced elastic stiffening of ZnO nanostructures: Skin-depth," Sens. Actuators **134** (2008) 353-1042.

[18] Y. Liu, L. Zhong, Z. Peng, Y. Song, W. Chen" Field emission properties of one-dimensional single CuOnanoneedle by in situ microscopy," Journal of Materials Science **45**, 14 (2010) 3791–3796.

[19] M. K. Shrestha, C. M. Sorensen & K. J. Klabunde, "Synthesis of CuOnanorods, reduction of CuO into Cu nanorods and diffuse reflectance Measurements of CuO and Cu nanomaterials in the near infrared region,"J. Phys. Chem. C **114**,34 (2010) 14368-14376.

[20] S. Young, Y. Cho, H. Duk, "CuO, Nanotubes synthesized by the thermal oxidation of Cu nanowires," Bull. Korean Chem. Soc **29** (2008) 2525-2527.

[21] A. Ananth, D. Subramanian, H. Moon-Soo, S. M. Young, "Copper oxide nanomaterials: Synthesis, characterization and structure-specific antibacterial performance," Chem. Eng. J. **262** (2015) 179-188.

[22] H. Zafar, I. bupoto, K. Kimleang, B. Valerio, L. Xianjie, W. Magnus, "Synthesis of Novel CuONanosheets and Their Non-Enzymatic Glucose Sensing Applications," Sensors **13** (2013) 7926-7938.

[23] X. Gou, G. J. Wang, J. Yang, D. Park Wexler, "Chemical synthesis, characterization and gas sensing performance of copper oxide nanoribbons,"J. Mater. Chem **18** (2008) 965-969.

[24] Z. Liao, B. Zhang, Z. Yan, Q. L. Zheng, T. Bao, C. M. Wu, Z. X. Li, J. X. Shen, H. Zhang, J. C. Gong, T. Y. Li," Multifunctional CuO nanowire devices: p-type field effect transistors and CO gas sensors," Nanotechnology **20** (2009) 1-6.

[25] D. Li, J. Hu, R. Wu & Jia G. L., "Conductometric chemical sensor based on individual CuO nanowires," Nanotechnology **21**, 48 (2010) 485502.

[26] Y. H. Ko, G.Nagaraju & J. S. Yu, "Facile preparation and optoelectronic properties of CuO nanowires for violet light sensing," Mater. Lett. **117** (2014) 217-220.

[27] L. -B. Luo, H. W. Xian, X. Chao, L. I. Zhong-Jun, Y. Xiao- Bao, L. u. Jian, "One-dimensional CuO nanowire: synthesis, electrical and optoelectronic devices application," Nanoscale Res. Lett. **9** (2014) 1-8.

[28] K. S. Wanjala, W. K. Njoroge, N. E. Makori, J. M. Ngaruiya, "Optical and electrical characterization of CuO thin films as absorber material for solar cell applications," Am. J. of Cond. Matter.Phys. **6** (2016) 1-6.

[29] S. B. Wanga, C. H. Hsiaoa, S. J. Changa, K. T. Lamb, K. H. Wenb, S. C. Hung, S. J. Young, B. R. Huang," A CuO nanowire infrared photodetector" Sens. and Actuators A **171** (2011) 207-211.

[30] A. Abdelrahim, Z. Huichao, Q. Xiaotong, C. Haitao, W. Xiaojiao, T. Zhenan, "Ultrahigh responsivity UV/IR photodetectors based on pure CuO nanowires," AIP Conf. Proceedings **1586** (2014) 92-96.

[31] Abdelrahim Ate, Huichao Zhu, Xiaotong Quan, Haitao Cai, Xiaojiao Wang & Zhenan Tang, "Ultrahigh responsivity UV/IR photodetectors based on pure CuO nanowires," AIP Conference Proceedings **1586**, 92 (2014).

[32] S Arya, A Sharma, B Singh, M Riyas, P Bandhoria, M Aatif, V Gupta, "sol-gel synthesis of Cu doped p-CdS NPs and their analysis as P-CdS / n-ZnO thin film photodiode," Opt. Mater. **79** (2018) 115-119.

[33] A. A. Al Ghamdi, A. Dere, A. Tataroğlu, B. A. F. Yakuphanoglu, F. El-Tantawy,W. A. Farooq, "Composite metal oxide semiconductor-based photodiodes for solar panel tracking applications," J. of Alloys and Comp. **650** (2015) 692-699.

[34] A. Mekki, R.O. Ocaya, A. Dere, A. A. Al Ghamdi, K. Harrabi, F. Yakuphanoglu, "New photodiodes based graphene-organic semiconductor hybrid materials," Synth. Met. **213** (2016) 47-56.

[35] N. F. Mott, E. A. Davies, Electronic Processes in Non-Crystalline Materials, Clarendon Press: Oxford, (1979).

[36] A. N. Banerjee, K. K. Chattopadhyay, D. Depla, S. Maheiu, Reactive Sputter Deposition 465, Springe:Verlag Berlin Heidelberg, (2008).

[37] I. A. Ezenwa & A. J Ekpunobi, "Optical properties and band offsets of CdS/ZnSsuperlattice deposited by chemical bath", J. of Non-Oxide Glasses **3** (2011) 77-87.

[38] T. H. Darma, A. A. Ogwu & F. Placido, "Effects of sputtering pressure on properties of copper oxide thin films prepared by rf magnetron sputtering," Mater. Technol. **26**, 1 (2011) 28-31.

[39] S. M. Dhanya, Shailendra Kumar, R. J. Choudhary, D. W. Avinash, K. J Mahaveer & A. Subrahmanyam, "Synthesis of Cu_2O from CuO thin films: Optical and electrical properties" AIP Advances **5** (2015) 1-5.

[40] S. B. Wang, C. H. Hsiao, S. J. Chang, K. T. Lam, K. H. Wen, S. C. Hung, S. J. Young, B. R. Huang, "A CuO nanowire infrared photodetector," Sens. and Actuators **171**, 2 (2011) 207-211.

[41] P. Wu, Y. Dai, Y. Ye, Y. Yin, L. Dai, "Fast-speed and high-gain photodetectors of individual single-crystalline Zn_3P_2 nanowires," J. Mater.Chem. **21**, 8 (2011) 2563-2567.

[42] A. Rose,Concepts in Photoconductivity and Allied Problems, Krieger Publishing company: New York, (1978).

[43] Y. Yu, Y. Jiang, K. Zheng, Z. Zhu, X. Zheng Lan, Y. Zhang, Y. Zhang & X. Xuan, "Ultralow-voltage and high gain photoconductor based on ZnS:Ga nanoribbons for the detection of low-intensity ultraviolet light,"J. Mater. Chem C **2** (2014) 3583-3588.

[44] L. Li, P.C. Wu, X. Fang, T. Zhai, L. Dai, M. Liao, Y. Koide, H. Wang, Y. Bando, D. Golberg, "Single-crystalline CdSnanobelts for excellent field-emitters and ultrahigh quantum-efficiency photodetectors," Adv. Mater. **22**, 29 (2010) 3161-3165.